KPZ- and Related Behavior of Hydrodynamics in One Dimension

Henk van Beijeren

Institute for Theoretical Physics
Utrecht University

Universiteit Utrecht

1) Problems with hydrodynamics in 1 and 2 dimensions.

2) The fluctuating Burgers equation
   a) Mode coupling results
   b) Exact results by Prähofer and Spohn

3) Hydrodynamics in one dimension.
   a) Mode coupling expansions
   b) Dominance of Prähofer-Spohn terms for long times
   c) Explicit results

4) Concluding remarks

Hydrodynamics in 1 and 2 dimensions is known since the 1960's to be plagued by divergence problems. Transport coefficients in linearized hydrodynamic equations are given by Green-Kubo expressions, such as

$$D = \frac{1}{d}\int_0^\infty dt \langle \boldsymbol{v}(0)\cdot \boldsymbol{v}(t)\rangle .$$

Assuming regular diffusion of mass and of momentum one finds that the average velocity of the tagged particle at time *t*, given it started out with velocity $\boldsymbol{v}_0$ is proportional to $\boldsymbol{v}_0\, t^{-d/2}$.

Universiteit Utrecht

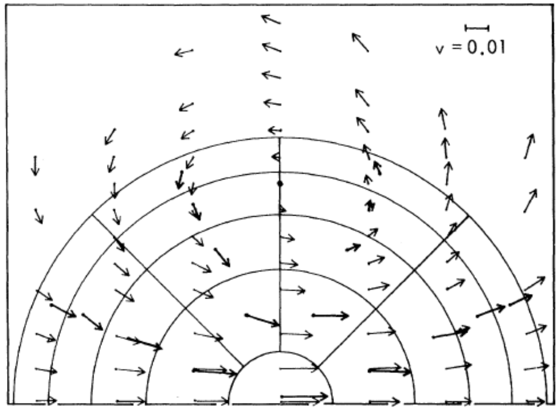

FIG. 1. Statistically averaged velocity field around a central disk from molecular dynamics (heavy arrows) compared to that given by the hydrodynamic model (light arrows). Because of symmetry only half the plane is shown. The scale of distance is indicated by the size of the central disk as shown by the smallest half-circle. The sizes of the other four concentric circles have been determined so as to include roughly six neighboring particles each. These semicircles have been partitioned further into four parts, as indicated by the lines, so as to have a measure of direction relative to the velocity vector of the central particle at zero time. The size of the arrows indicates the magnitude of the velocity (the scale of velocity is indicated as 0.01 of the initial velocity in the upper right-hand corner) and the direction of the arrow is determined by the parallel and perpendicular components of the velocity (relative to that of the central particle initially) averaged over all the particles in that section at a particular time. The arrow is hence drawn at the center of the section. A correction of $1/N-1$ has been added to the parallel component. The comparison is made at 9.9 collision times where the molecular-dynamic and hydrodynamic velocity autocorrelations begin to nearly agree, as seen on the graph by the velocity vectors of the central particle. (See also Fig. 3.) In the molecular-dynamics run, 224 hard disks were used at an area relative to close packing of 2. For the hydrodynamic run, the conditions are given in Table I.

hydrodynamic calculation. The late-time kinks seen in Fig. 3 in the velocity autocorrelation functions calculated for 504 particle systems are caused by the arrival of sound waves from the periodic images. The arrival time of these interferences can be predicted by the hydrodynamical model.

A simple analysis of the hydrodynamical model

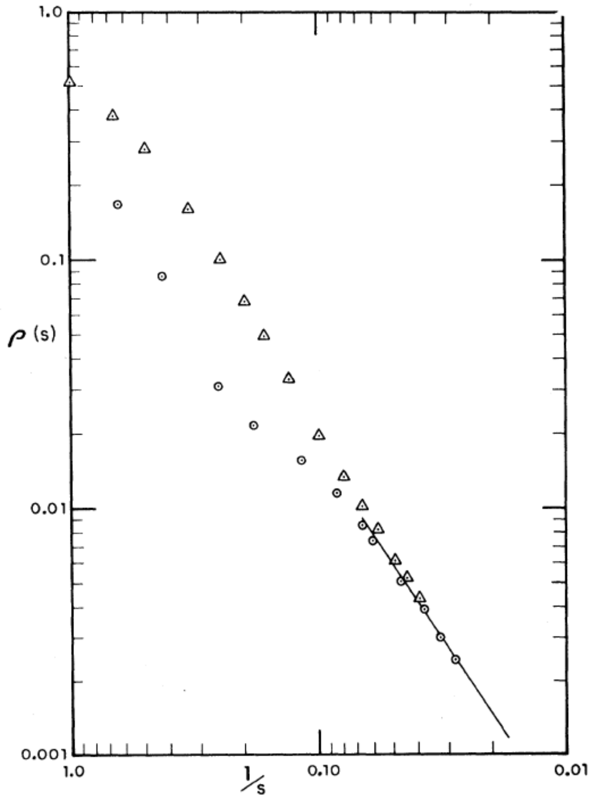

FIG. 2. Comparison of the velocity autocorrelation function $\rho(s)$ as a function of time (in terms of mean collision times s) between the hydrodynamic model (circles) and a 500-hard-sphere molecular-dynamic calculation (triangles) at a volume relative to close packing of 3 on a log-log plot. The straight line is drawn with a slope corresponding to $s^{-3/2}$. To the molecular dynamics $\rho(s)$

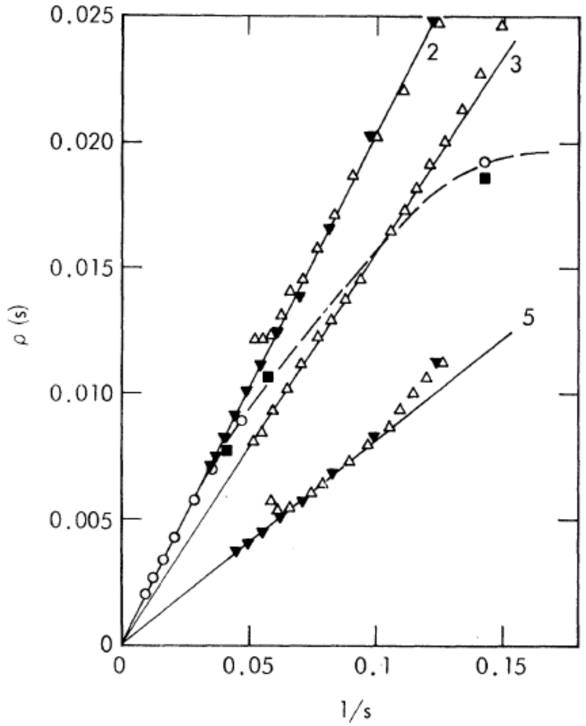

FIG. 3. The decay of the velocity autocorrelation function at large times for hard disks at three densities: $A/A_0 = 2, 3$, and 5. The closed and open triangles refer to molecular-dynamic runs of 986 and 504 particles, respectively. A $1/N - 1$ correction to the molecular-dynamic results has been applied. At A/A_0 of 2 and 5 the 504-particle results include the initial deviations due to the interference of neighboring cells at the boundary while all other results have not been plotted beyond the point where serious interference is indicated. The dashed line represents the results of a hydrodynamic run at A/A_0 of 2 (see Table I for conditions) in which the initially moving square area element was given two different velocities, the root-mean-square molecular velocity (squares) and that $\frac{1}{14}$th as large (circles).

Hydrodynamics in 1 and 2 dimensions is known since the 1960's to be plagued by divergence problems. Transport coefficients in linearized hydrodynamic equations are given by Green-Kubo expressions, such as

$$D = \frac{1}{d}\int_0^\infty dt \langle \boldsymbol{v}(0)\cdot\boldsymbol{v}(t)\rangle.$$

Assuming regular diffusion of mass and of momentum one finds that the average velocity of the tagged particle at time t, given it started out with velocity $\boldsymbol{v}(0)$ is proportional to $\boldsymbol{v}(0)\, t^{-d/2}$. The time integral of this diverges for $d = 1$ or 2.

Universiteit Utrecht

One can improve on this by using self-consistent theories. These predict:

$$< \upsilon(0)\cdot\upsilon(t) >\sim \frac{1}{t\sqrt{\ln t}} \quad (d=2)$$

$$< j(0)\,j(t) >\sim \frac{1}{t^{2/3}} \quad (d=1)$$

PHYSICAL REVIEW E **77**, 021201 (2008)

Long-time tail of the velocity autocorrelation function in a two-dimensional moderately dense hard-disk fluid

Masaharu Isobe*
Graduate School of Engineering, Nagoya Institute of Technology, Nagoya 466-8555, Japan
(Received 14 June 2007; revised manuscript received 16 November 2007; published 7 February 2008)

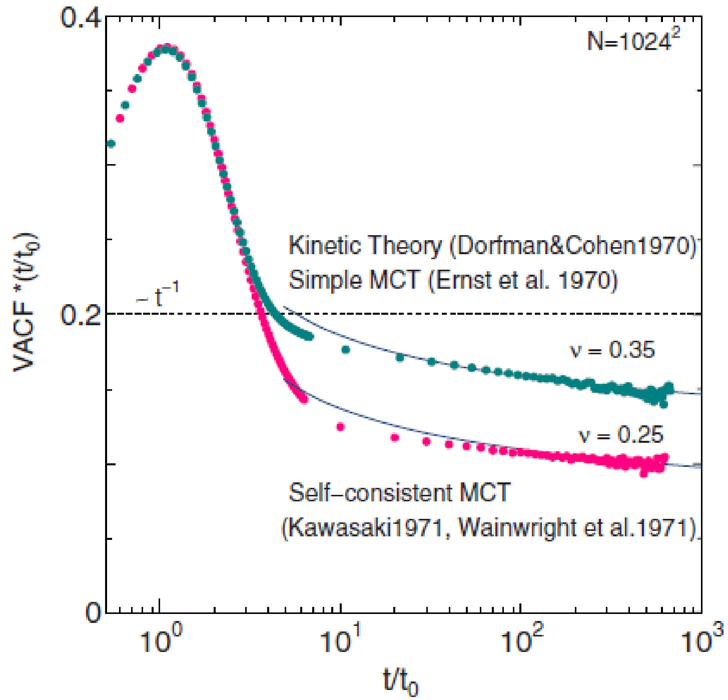

FIG. 5. (Color online) The VACFs in a moderately dense hard-disk fluid are compared between numerical simulations and the theoretical predictions using the simple MCT [6] (dashed line) and self-consistent MCT [14,15] (solid line).

Heat Conduction and Entropy Production in a One-Dimensional Hard-Particle Gas

Peter Grassberger, Walter Nadler, and Lei Yang
John-von-Neumann Institute for Computing, Forschungszentrum Jülich, D-52425 Jülich, Germany
(Received 13 March 2002; published 11 October 2002)

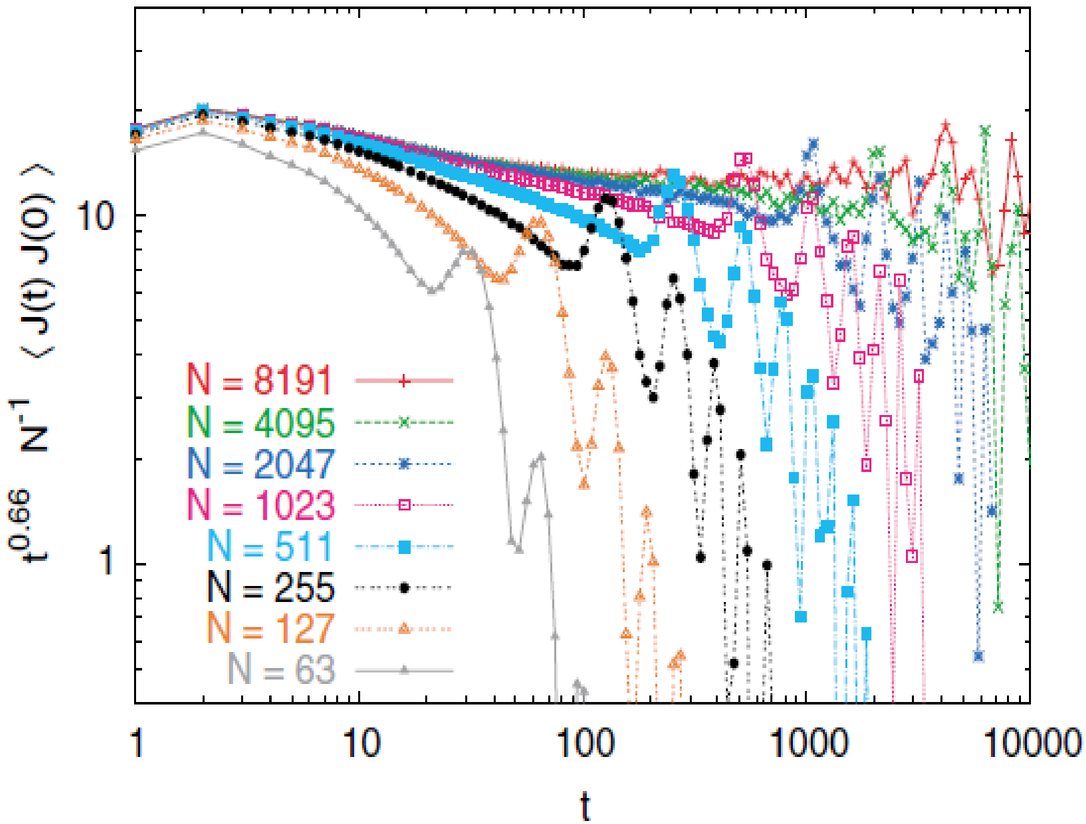

FIG. 4 (color). Total heat current autocorrelation, $t^{0.66}N^{-1}$ $\langle J(t)J(0)\rangle$ for $r = 2.2$ and $T = 2$. Total momentum is $P = 0$.

Fluctuating Burgers equation

$$\frac{\partial \phi(\boldsymbol{r},t)}{\partial t} = -\frac{\boldsymbol{w}}{2} \cdot \nabla \phi^2(\boldsymbol{r},t) + D\nabla^2\phi(\boldsymbol{r},t) - \nabla \cdot \boldsymbol{j}_L(\boldsymbol{r},t)$$

Can be used for describing driven, collective single file diffusion, traffic flows and ASEP's among other things.

Universiteit Utrecht

Fluctuating Burgers equation

$$\frac{\partial \phi(\boldsymbol{r},t)}{\partial t} = -\frac{\boldsymbol{w}}{2} \cdot \nabla \phi^2(\boldsymbol{r},t) + D\nabla^2 \phi(\boldsymbol{r},t) - \nabla \cdot \boldsymbol{j}_L(\boldsymbol{r},t)$$

For Fourier components:

$$\frac{\partial}{\partial t}\hat{\phi}(\boldsymbol{k},t) = -\frac{i\boldsymbol{k}\cdot\boldsymbol{w}}{2V}\sum_{\boldsymbol{q}} \hat{\phi}(\boldsymbol{q},t)\hat{\phi}(\boldsymbol{k}-\boldsymbol{q},t) - Dk^2\hat{\phi}(\boldsymbol{k},t) - i\boldsymbol{k}\hat{\jmath}_L(\boldsymbol{k},t)$$

May be rewritten into the integral equation

$$\begin{aligned}\hat{\phi}(\boldsymbol{k},t) &= e^{-Dk^2(t-t_0)}\hat{\phi}(k,t_0) - \int_{t_0}^{t} d\tau\, e^{-Dk^2(t-\tau)} i\boldsymbol{k}\cdot\hat{\jmath}_L(\boldsymbol{k},\tau) \\ &\quad - \int_{t_0}^{t} d\tau\, e^{-Dk^2(t-\tau)} \frac{i\boldsymbol{k}\cdot\boldsymbol{w}}{2V}\sum_{\boldsymbol{q}} \hat{\phi}(\boldsymbol{q},\tau)\hat{\phi}(\boldsymbol{k}-\boldsymbol{q},\tau)\end{aligned}$$

$$\hat{\phi}(\boldsymbol{k},t) = e^{-Dk^2(t-t_0)}\hat{\phi}(k,t_0) - \int_{t_0}^{t} d\tau\, e^{-Dk^2(t-\tau)} i\boldsymbol{k}\cdot\hat{\boldsymbol{j}}_L(\boldsymbol{k},\tau) - \int_{t_0}^{t} d\tau\, e^{-Dk^2(t-\tau)} \frac{i\boldsymbol{k}\cdot\boldsymbol{w}}{2V} \sum_{\boldsymbol{q}} \hat{\phi}(\boldsymbol{q},\tau)\hat{\phi}(\boldsymbol{k}-\boldsymbol{q},\tau)$$

One can iterate this equation and make a diagrammatic expansion for the time correlation function $\hat{S}(\boldsymbol{k},t-t_0) = \frac{1}{V} < \hat{\phi}(-\boldsymbol{k},t_0)\hat{\phi}(\boldsymbol{k},t) >$.

Diagrammatic elements:

$\underline{\quad\boldsymbol{q}\quad}$ representing factors $e^{-Dq^2(\tau_j-\tau_{j-1})}$

vertices 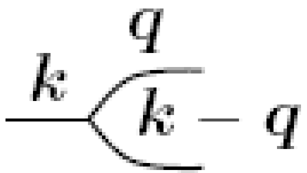

representing factors $\frac{i\boldsymbol{k}\cdot\boldsymbol{w}}{2V} \int_{\tau_{j-1}}^{t} d\tau_j \sum_{\boldsymbol{q}}$

$\bullet \rightarrow \hat{\phi}(\boldsymbol{q},t_0)$ $\quad * \rightarrow \int d\tau\,[-i\boldsymbol{q}\cdot\hat{\boldsymbol{j}}_L(\boldsymbol{q},\tau)]$

$$\hat{\phi}(\boldsymbol{k},t) = e^{-Dk^2(t-t_0)}\hat{\phi}(k,t_0) - \int_{t_0}^{t} d\tau\, e^{-Dk^2(t-\tau)} i\boldsymbol{k}\cdot\hat{\boldsymbol{j}}_L(\boldsymbol{k},\tau)$$

$$- \int_{t_0}^{t} d\tau\, e^{-Dk^2(t-\tau)} \frac{i\boldsymbol{k}\cdot\boldsymbol{w}}{2V} \sum_{\boldsymbol{q}} \hat{\phi}(\boldsymbol{q},\tau)\hat{\phi}(\boldsymbol{k}-\boldsymbol{q},\tau)$$

$< \hat{\phi}(-\boldsymbol{k},t_0)\hat{\phi}(\boldsymbol{k},t) > =$

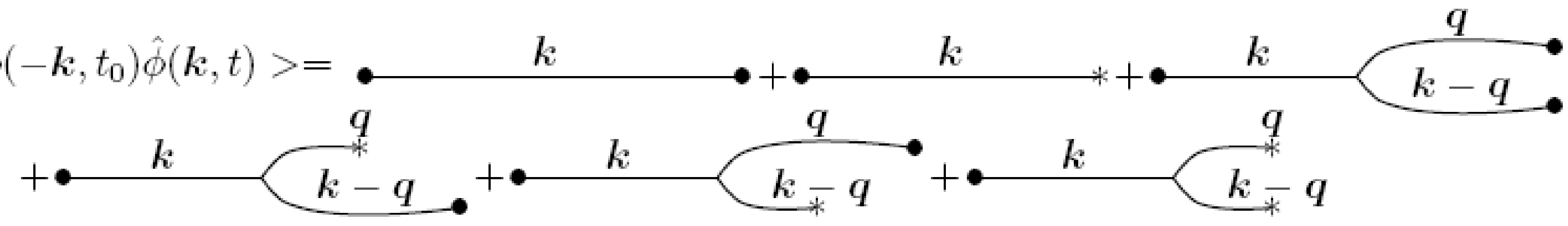

$+ \cdots$

$$\equiv \hat{S}(k, t - t_0)$$

Next iteration:

$$< \hat{\phi}(-\boldsymbol{k}, t_0)\hat{\phi}(\boldsymbol{k}, t) >=$$

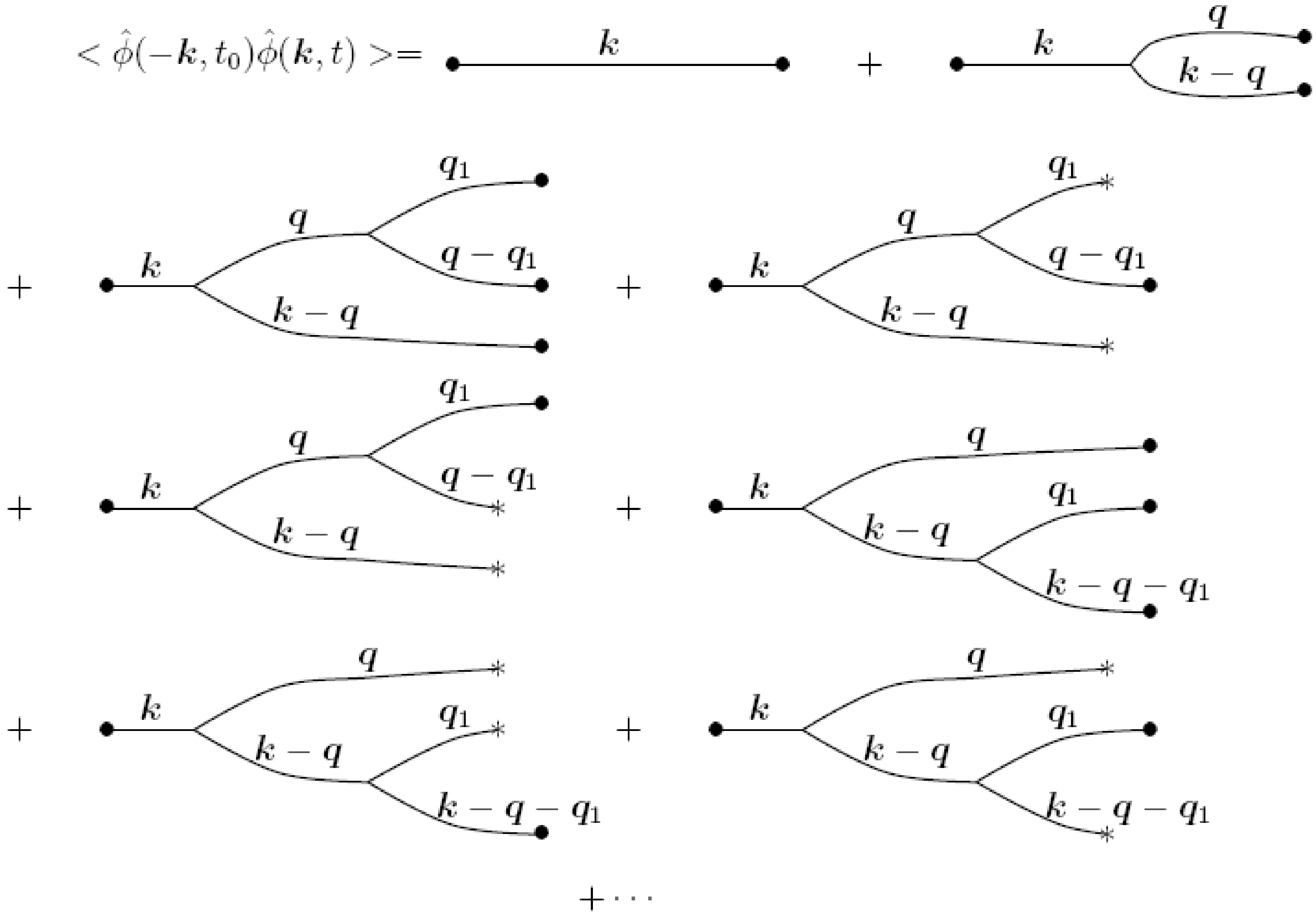

Assume the fluctuating current may be represented as Gaussian white noise with variance given in Fourier representation by

$$\frac{1}{V}\left\langle \hat{\boldsymbol{j}}_L(\boldsymbol{q},t)\hat{\boldsymbol{j}}_L(\boldsymbol{q}',t')\right\rangle = 2D\hat{S}(\boldsymbol{q})\delta(\boldsymbol{q}+\boldsymbol{q}')\delta(t-t')\mathbf{1},$$

with $\hat{S}(\boldsymbol{q}) \equiv \hat{S}(\boldsymbol{q}, t=0)$.

Assuming that n-point equal time density correlation functions in the stationary state may be factorized into products of two-point correlation functions, one may simplify the diagrams by using the identity

$$e^{-2Dk^2t}\hat{S}(\boldsymbol{k}) + \frac{1}{V}\int_0^t d\tau_1 \int_0^t d\tau_2 e^{-Dk^2(\tau_1+\tau_2)} < \hat{\boldsymbol{j}}_L(\boldsymbol{k},\tau_1)\hat{\boldsymbol{j}}_L(-\boldsymbol{k},\tau_2) >= \hat{S}(\boldsymbol{k})\mathbf{1},$$

For example:

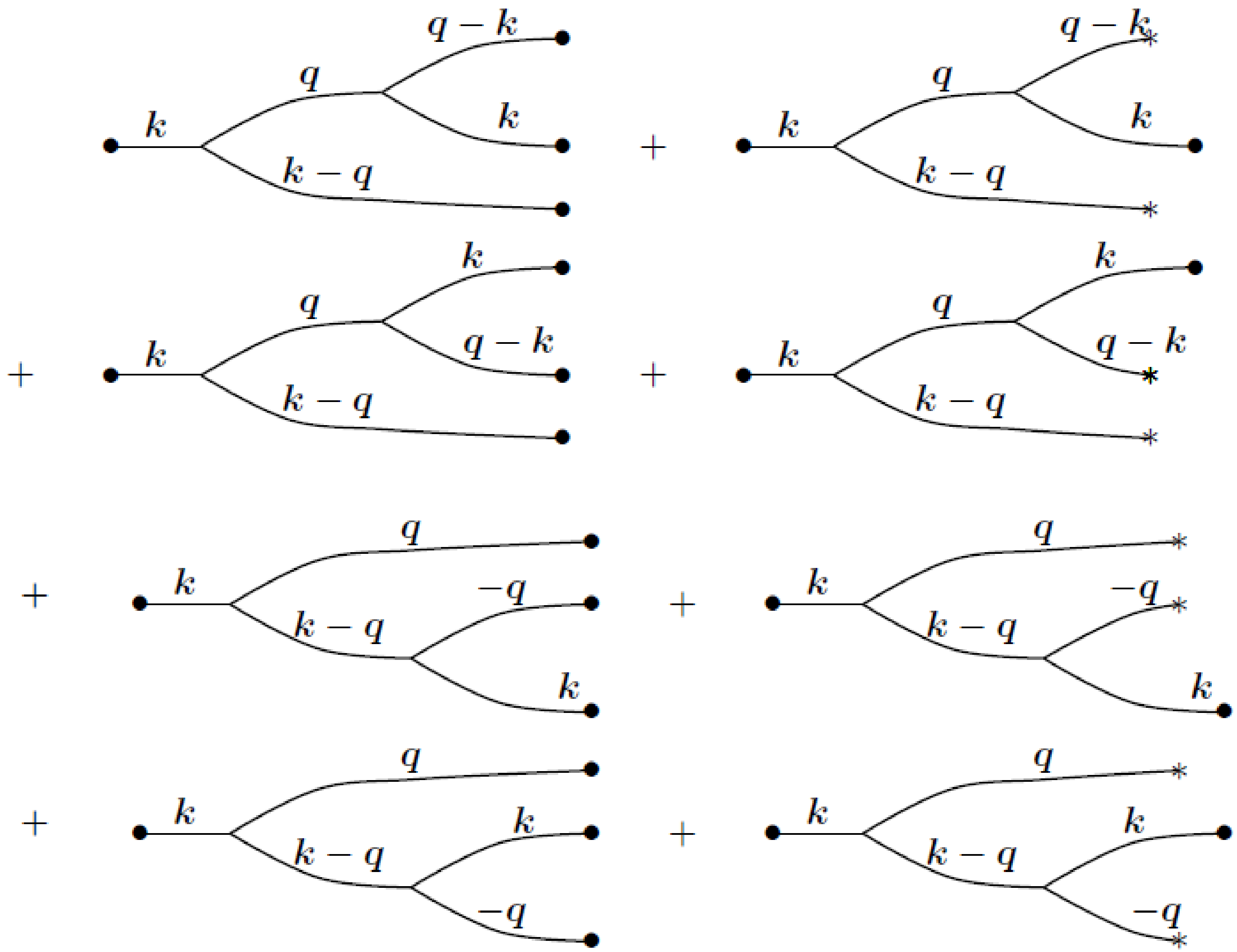

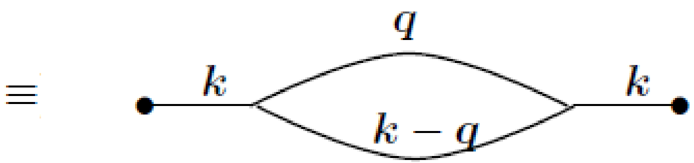

with right vertex weight:

$$2i\boldsymbol{k}\cdot\boldsymbol{w}\,\hat{S}(0)\int_0^{\tau_1} d\tau_2.$$

$$\frac{1}{V}\langle \hat{\boldsymbol{j}}_L(\boldsymbol{q},t)\hat{\boldsymbol{j}}_L(\boldsymbol{q}',t')\rangle = 2D\hat{S}(\boldsymbol{q})\delta(\boldsymbol{q}+\boldsymbol{q}')\delta(t-t')\mathbf{1}$$

with $\hat{S}(k) \equiv \hat{S}(k,0)$

$$\rightarrow e^{-2Dk^2t}\hat{S}(\boldsymbol{k}) + \int_0^t d\tau_1 \int_0^t d\tau_2 e^{-Dk^2(\tau_1+\tau_2)}\boldsymbol{k}\boldsymbol{k}\colon < \hat{\boldsymbol{j}}_L(\boldsymbol{k},\tau_1)\hat{\boldsymbol{j}}_L(-\boldsymbol{k},\tau_2) >= \hat{S}(\boldsymbol{k}),$$

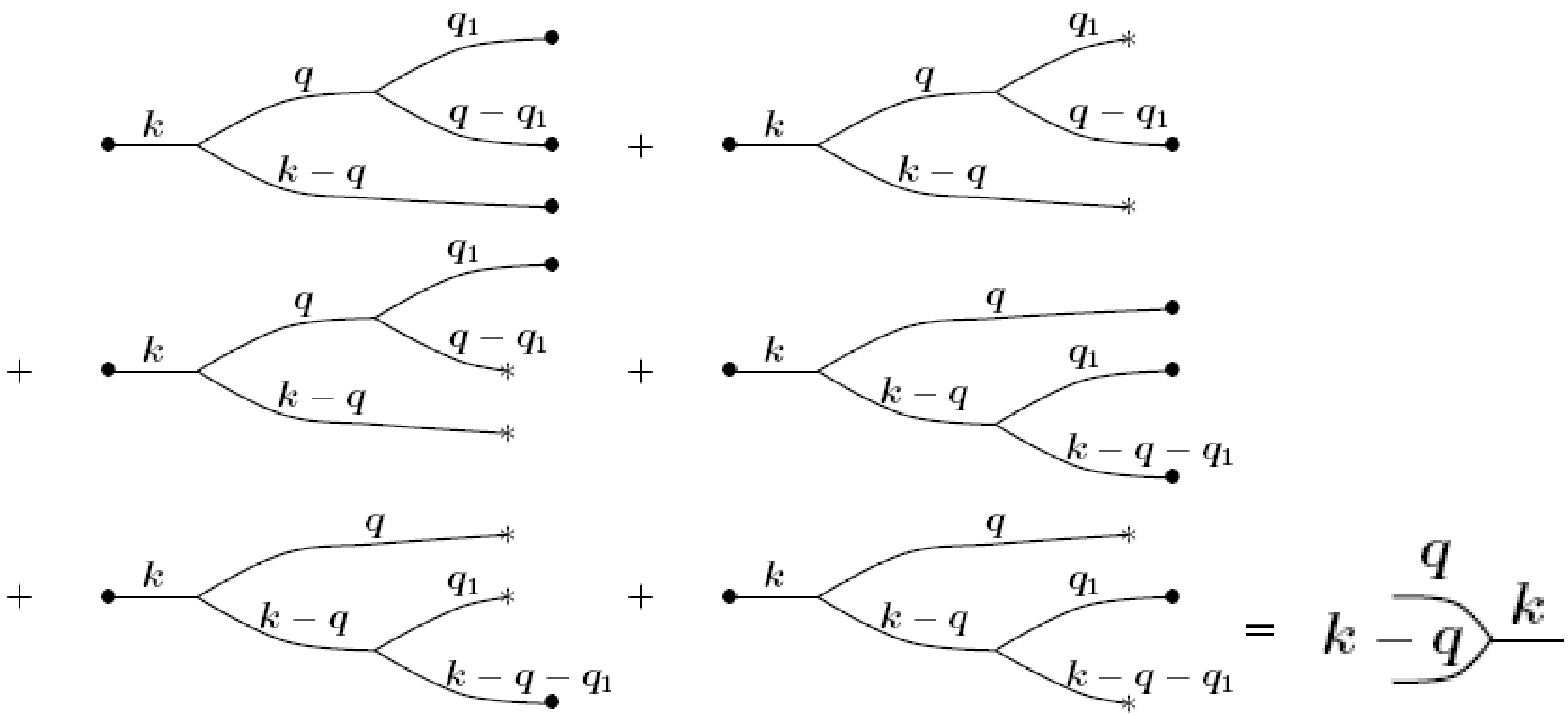

with vertex weight $2i\boldsymbol{k}\cdot\boldsymbol{w}\,\hat{S}(0)\int_0^{\tau_1} d\tau_2$

Applying the same reductions to the full diagrammatic expansion of $\hat{S}(\boldsymbol{k},t)$ one obtains

$\hat{S}(\boldsymbol{k},t) =$

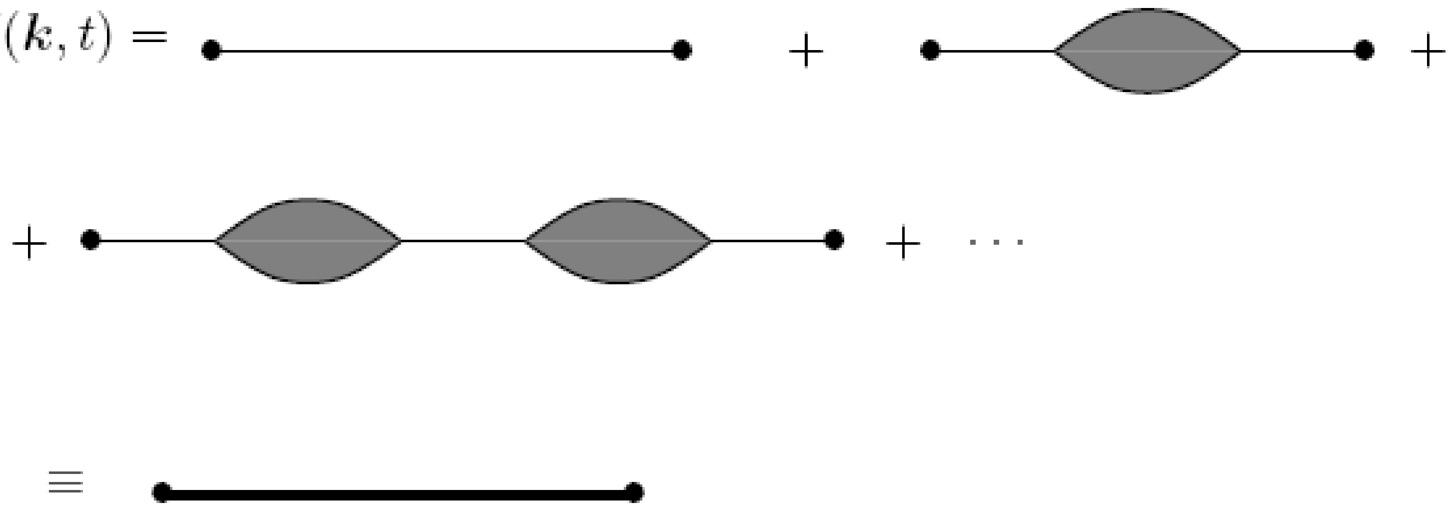

Diagrammatic mode coupling expansion leads to Dyson structure:

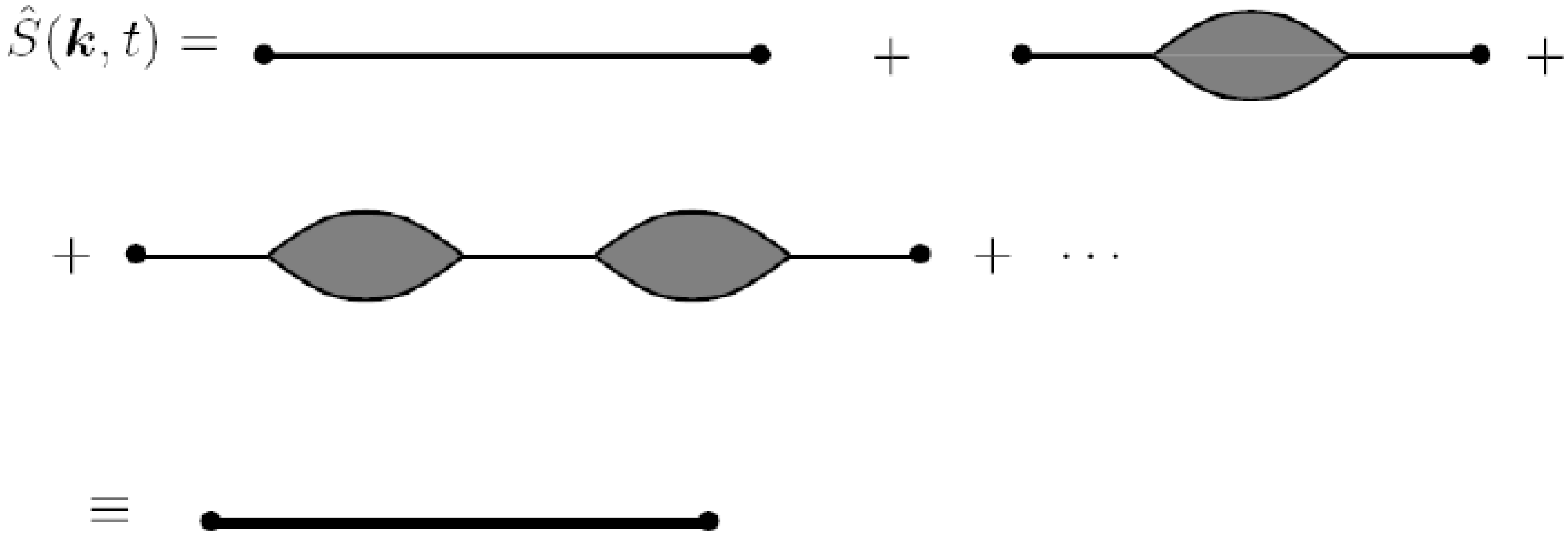

Applying the same reductions to the full diagrammatic expansion of $\hat{S}(\boldsymbol{k},t)$ one obtains

$\hat{S}(\boldsymbol{k},t) =$

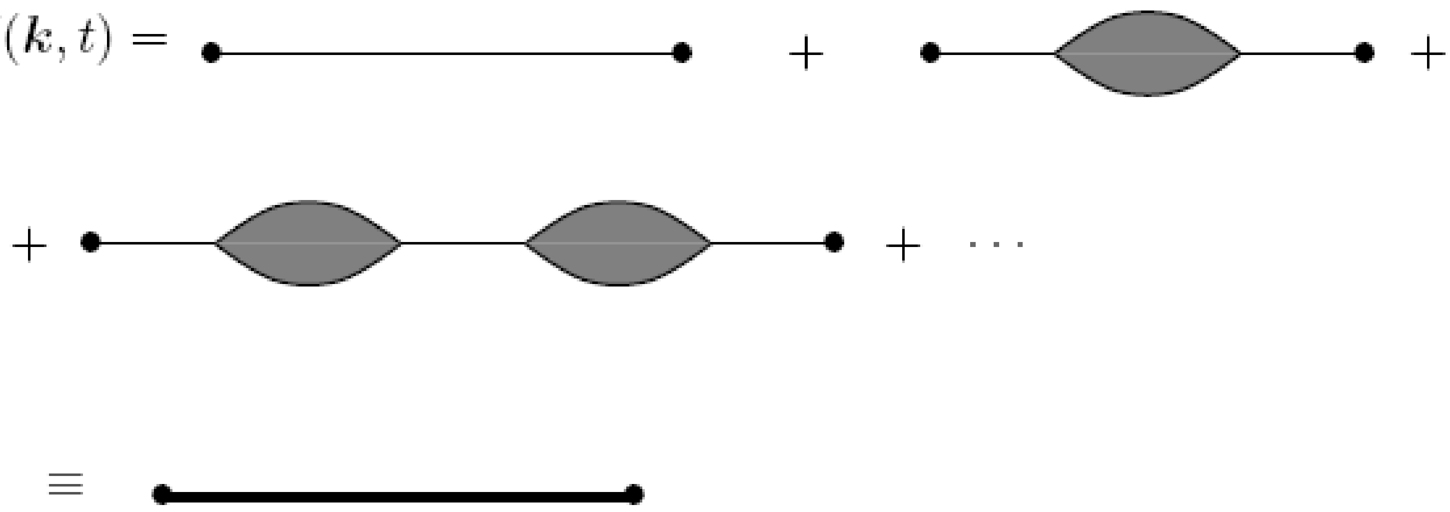

A skeleton renormalization gives:

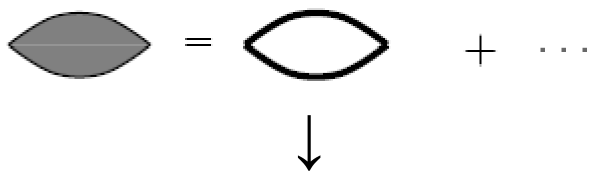

Keeping only this leads to a one-loop mode coupling approximation.

$\hat{S}(\boldsymbol{k}, t) =$

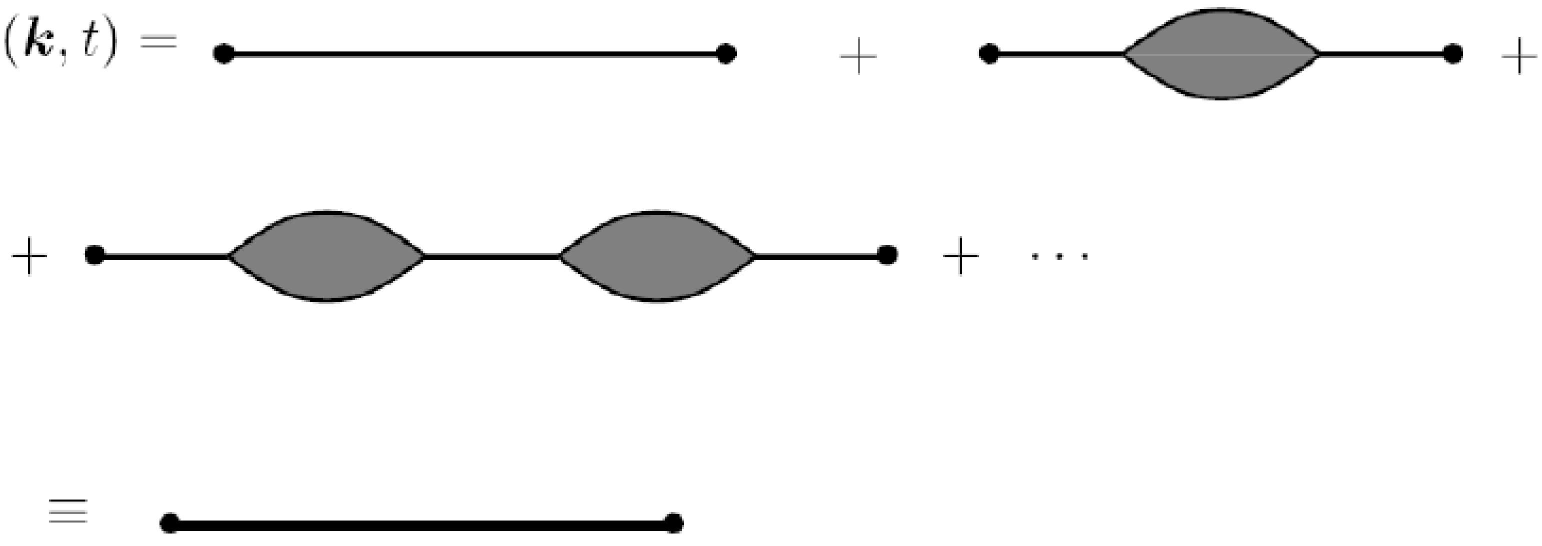

A skeleton renormalization gives:

Keeping only this leads to a one-loop mode coupling approximation.

$$\frac{\partial \hat{S}(\boldsymbol{k},t)}{\partial t} = -Dk^2\hat{S}(\boldsymbol{k},t) - \frac{(\boldsymbol{w}\cdot\boldsymbol{k})^2}{2\hat{S}(\boldsymbol{0})V}\int_0^{t-t_0} d\tau \sum_{\boldsymbol{q}} \hat{S}(\boldsymbol{q},\tau)\hat{S}(\boldsymbol{k}-\boldsymbol{q},\tau)\hat{S}(\boldsymbol{k},t-\tau),$$

where again all equal-time correlation functions have been approximated by $\hat{S}(0)$. Notice that in the limit $V \to \infty$, $\frac{1}{V}\sum_{\boldsymbol{q}}$ approaches $\frac{1}{(2\pi)^d}\int d\boldsymbol{q}$.

The Green-Kubo formalism relates the time derivative of $\hat{S}(\boldsymbol{k},t)$ to a current-current time correlation function

$$\frac{\partial}{\partial t}\hat{S}(\boldsymbol{k},t) = -k^2\int_0^{\infty} d\tau\, \hat{M}(\boldsymbol{k},\tau)\hat{S}(\boldsymbol{k},t-\tau)$$

with

$$\lim_{k\to 0}\hat{M}(\boldsymbol{k},\tau) = \hat{\boldsymbol{k}}\hat{\boldsymbol{k}} : \left\langle \left(\boldsymbol{J}(0) - <\boldsymbol{J}(0)> - \frac{\partial J(\bar{c})}{\partial \bar{c}}(N(0) - <N>)\right) \cdot \left(\boldsymbol{J}(t) - <\boldsymbol{J}> - \frac{\partial J(\bar{c})}{\partial \bar{c}}(N(t) - <N>)\right)\right\rangle.$$

On the other hand, in one-loop MC approximation:

$$M(\boldsymbol{k},t) = D\delta(t) + \frac{(\boldsymbol{w}\cdot\hat{\boldsymbol{k}})^2}{2\hat{S}(0)V}\sum_{\boldsymbol{q}}\hat{S}(\boldsymbol{q},t)\hat{S}(\boldsymbol{k}-\boldsymbol{q},t).$$

For d>2, $\hat{S}(\boldsymbol{k},t)$ may be approximated by $\hat{S}(0)e^{-Dk^2t}$. →

$$M(\boldsymbol{k},t) = \frac{(\boldsymbol{w}\cdot\hat{\boldsymbol{k}})^2\hat{S}(0)}{2(8\pi Dt)^{d/2}} \qquad t \text{ large}$$

For d = 1,2 the mode coupling term dominates

$$\frac{\partial \hat{S}(\boldsymbol{k},t)}{\partial t} = -Dk^2\hat{S}(\boldsymbol{k},t) - 2\frac{(\boldsymbol{w}\cdot\boldsymbol{k})^2}{\hat{S}(\mathbf{0})V}\int_0^{t-t_0} d\tau \sum_{\boldsymbol{q}} \hat{S}(\boldsymbol{q},\tau)\hat{S}(\boldsymbol{k}-\boldsymbol{q},\tau)\hat{S}(\boldsymbol{k},t-\tau)$$

For $d = 1, 2$ the mode coupling terms dominate the diffusion equation. To analyze this for $d = 1$, first introduce dimensionless variables: $\tau = \alpha t$; $\kappa = \beta k$;

$$\Sigma(\kappa,\tau) = \frac{\hat{S}(\frac{\kappa}{\beta},\frac{\tau}{\alpha})}{\hat{S}(0)} \text{ with } \alpha = \frac{w^4 S^2(0)}{128 D^3} \quad \beta = \frac{16D^2}{w^2\hat{S}(0)} \Rightarrow$$

$$\frac{\partial \Sigma(\kappa,\tau)}{\partial \tau} = -\frac{1}{2}\kappa^2\left[\Sigma(\kappa,t) + \frac{2}{\pi}\int_0^{\tau} d\sigma \int_{-\infty}^{\infty} d\lambda\, \Sigma(\lambda,\sigma)\Sigma(\kappa-\lambda,\sigma))\Sigma(\kappa,\tau-\sigma)\right]$$

Assume: $\Sigma(\kappa,\tau) = h(\kappa\tau^{\alpha})$, with $h(0) = 1$

Universiteit Utrecht

$$\frac{\partial \hat{S}(\boldsymbol{k},t)}{\partial t} = -Dk^2\hat{S}(\boldsymbol{k},t) - 2\frac{(\boldsymbol{w}\cdot\boldsymbol{k})^2}{\hat{S}(\boldsymbol{0})V}\int_0^{t-t_0} d\tau \sum_{\boldsymbol{q}} \hat{S}(\boldsymbol{q},\tau)\hat{S}(\boldsymbol{k}-\boldsymbol{q},\tau)\hat{S}(\boldsymbol{k},t-\tau)$$

For $d = 1, 2$ the mode coupling terms dominate the diffusion equation. To analyze this for $d = 1$, first introduce dimensionless variables: $\tau = \alpha t$; $\kappa = \beta k$;

$$\Sigma(\kappa,\tau) = \frac{\hat{S}(\frac{\kappa}{\beta},\frac{\tau}{\alpha})}{\hat{S}(0)} \text{ with } \alpha = \frac{w^4 S^2(0)}{128 D^3} \quad \beta = \frac{16D^2}{w^2\hat{S}(0)} \Rightarrow$$

$$\frac{\partial \Sigma(\kappa,\tau)}{\partial \tau} = -\frac{1}{2}\kappa^2\left[\Sigma(\kappa,t) + \frac{2}{\pi}\int_0^\tau d\sigma \int_{-\infty}^{\infty} d\lambda\, \Sigma(\lambda,\sigma)\Sigma(\kappa-\lambda,\sigma))\Sigma(\kappa,\tau-\sigma)\right]$$

Assume: $\Sigma(\kappa,\tau) = h(\kappa\tau^{\alpha})$, with $h(0) = 1 \quad \rightarrow$

$$\Sigma(\kappa,\tau) = h(\kappa\tau^{2/3})$$

$$< J(0)J(t) > \sim t^{-2/3}$$

$$D(k) = \int_0^\infty dt\; M(k,t) \sim k^{-1/2}$$

The Kardar-Parisi-Zhang equations

By integrating the 1d fluctuating Burgers equation over *x* one obtains the 1d KPZ equation:

$$\frac{\partial \phi(\boldsymbol{r},t)}{\partial t} = -\frac{\boldsymbol{w}}{2} \cdot \nabla \phi^2(\boldsymbol{r},t) + D\nabla^2 \phi(\boldsymbol{r},t) - \nabla \cdot \boldsymbol{j}_L(\boldsymbol{r},t)$$

$$\frac{\partial h(x,t)}{\partial t} = D\frac{\partial^2 h(x,t)}{\partial x^2} - \frac{w}{2}\left(\frac{\partial h(x,t)}{\partial x}\right)^2 + \eta_L(x,t)$$

Prähofer and Spohn found an exact solution for the polynuclear growth model, which belongs to the KPZ universality class.

Main results of PS, translated to the fluctuating Burgers equation:

$$\frac{1}{L} < \tilde{J}(t)\tilde{J}(0) > = \frac{2.1056}{\sqrt{3}\Gamma_E(1/3)} \left(\frac{\hat{S}(0)w^2}{4t} \right)^{2/3}$$

$$D(k) = \frac{8}{19.444} \sqrt{\frac{2\hat{S}(0)w^2}{|k|}}.$$

Exact scaling functions were obtained for the density-density correlation function Ŝ(k,t) (or S(x,t)).

Main results of PS, translated to the fluctuating Burgers equation:

$$\frac{1}{L} < \tilde{J}(t)\tilde{J}(0) >= \frac{2.1056}{\sqrt{3}\Gamma_E(1/3)} \left(\frac{\hat{S}(0)w^2}{4t^2} \right)^{2/3}$$

$$D(k) = \frac{8}{19.444} \sqrt{\frac{2\hat{S}(0)w^2}{|k|}}.$$

In fact their results contain exactly known scaling functions for arbitrary combinations of small *k,* long times or small frequencies.

Fluctuating hydrodynamics in one dimension

$$\frac{\partial \rho(x,t)}{\partial t} = -\frac{\partial}{\partial x}[\rho(x,t)u(x,t)]$$

$$\rho\left(\frac{\partial}{\partial t} + u(x,t)\frac{\partial}{\partial x}\right)u(x,t) = -\frac{\partial p(x,t)}{\partial x} + \frac{\partial}{\partial x}\left\{\zeta(n(x,t),T(x,t))\frac{\partial u(x,t)}{\partial x}\right\} + \frac{\partial \sigma^r(x,t)}{\partial x}$$

$$\rho(x,t)T(x,t)\left(\frac{\partial}{\partial t} + u(x,t)\frac{\partial}{\partial x}\right)s(x,t) = \zeta(n(x,t),T(x,t))\left(\frac{\partial u(x,t)}{\partial x}\right)^2 +$$

$$+\sigma^r(x,t)\frac{\partial u(x,t)}{\partial x} + \frac{\partial}{\partial x}\left(\lambda(x,t)\frac{\partial T(x,t)}{\partial x}\right) - \frac{\partial q^r(x,t)}{\partial x}. \qquad 177)$$

with

$$\frac{\partial p(x,t)}{\partial x} = \left(\frac{\partial p}{\partial e}\right)_n \frac{\partial e(x,t)}{\partial x} + \left(\frac{\partial p}{\partial n}\right)_e \frac{\partial n(x,t)}{\partial x}$$

and derivatives of $s(x,t)$ and $T(x,t)$ defined in similar way

Linearization plus Fourier transform gives

$$\frac{\partial \hat{n}(k,t)}{\partial t} = -ikn_0\hat{u}(k,t),$$

$$\rho_0\frac{\partial \hat{u}(k,t)}{\partial t} = -ik\hat{p}(k,t) + ik\left[ik\zeta_0\hat{u}(k,t) + \hat{\sigma}^r(k,t)\right]$$

$$T_0\frac{\partial \hat{s}(k,t)}{\partial t} = -\frac{\lambda_0}{\rho_0}k^2\hat{T}(k,t) - \frac{ik}{\rho_0}q^r(k,t).$$

Diagonalizing gives three hydrodynamic modes,

$$a_\sigma(k,t) = \left(\frac{\beta}{2\rho_0}\right)^{1/2}\left(c_0^{-1}p(k,t) + \sigma g(k,t)\right), \quad \sigma = \pm 1; \quad \nu = -\sigma i c_0 k - \tfrac{1}{2}\Gamma k^2$$

$$a_H(k,t) = \left(\frac{\beta}{n_0T_0C_p}\right)^{1/2}\left(e(k,t) - h_0 n(k,t)\right) \quad \nu = -\frac{\lambda_0}{nc_p}k^2 = -D_T k^2$$

The time correlation functions of the hydrodynamic modes satisfy linear equations involving memory kernels, of similar form as the density-density time correlation function for the Burgers equation.

$$\frac{\partial \hat{S}_\sigma(k,t)}{\partial\, t} = -i\sigma c_0 k \hat{S}_\sigma(k,t) - k^2 \int_0^t d\tau \hat{M}_\sigma(k,\tau)\hat{S}_\sigma(k,t-\tau)$$

$$\frac{\partial \hat{S}_H(k,t)}{\partial\, t} = -k^2 \int_0^t d\tau \hat{M}_H(k,\tau)\hat{S}_H(k,t-\tau).$$

Like for the fluctuating Burgers equation the memory kernels may be expressed through a diagrammatic mode coupling expansion, but now there are three types of lines, corresponding to the three types of hydrodynamic modes and 27 vertices, corresponding to all combinations of lines coming in and running out.

Crucial observation: Due to different propagation speeds of different types of modes internally only couplings of a mode σ to two modes with the same value of σ contribute to the dominant long time behavior.

Therefore, in a comoving frame the sound-sound time correlation functions to leading order are of the same form as the Burgers density-density time correlation function.

Leading long-time and small wave number results:

$$S_\sigma(k,t) = \exp(-i\sigma ckt)\, f_{PS}[(\sqrt{2}V_\sigma^{\sigma\sigma})^{2/3} kt]$$

$$\Gamma(k) = \frac{8\sqrt{2}\ V_\sigma^{\sigma\sigma}}{19.444\ k^{1/2}} \qquad V_\sigma^{\sigma\sigma} = \frac{\sigma}{2(\rho\beta)^{1/2} c_0}\left(\frac{\partial c_0 n}{\partial n}\right)_S$$

$$\frac{1}{L}\langle J_\sigma(0) J_\sigma(t)\rangle = \frac{3}{5\pi}\Gamma_E\left(\frac{3}{5}\right)\frac{(V_\sigma^{HH})^2}{V_H^{\sigma\sigma}}\left(\frac{2c\ (V_\sigma^{\sigma\sigma})^2}{1.0528 V_H^{\sigma\sigma}}\right)^{1/5} t^{-3/5}$$

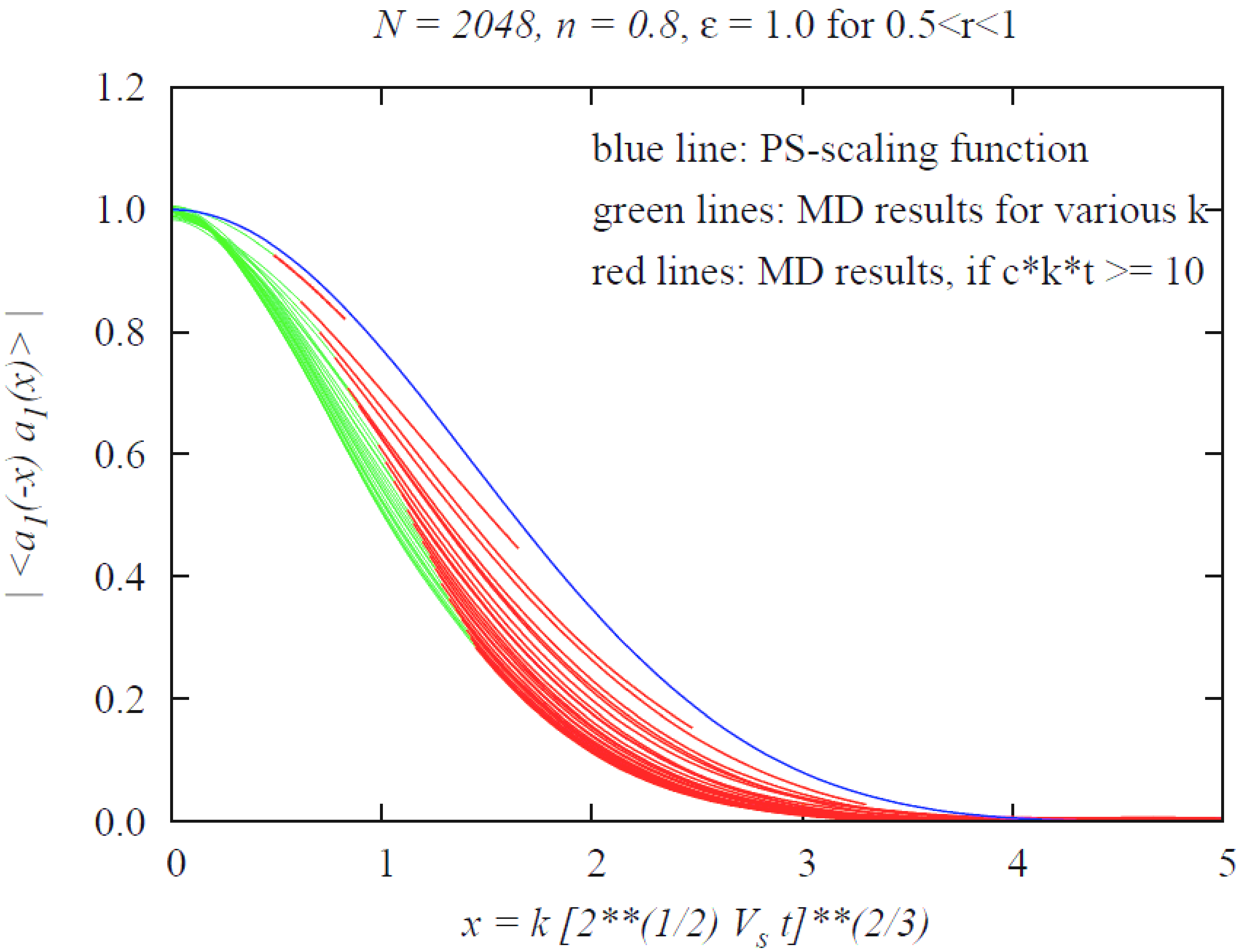

N = 2048, n = 0.8, ε = 1.0 for 0.5<r<1
blue line: PS-scaling function
green lines: MD results for various k
red lines: MD results, if c*k*t >= 10
| <a1(-x) a1(x)> |
x = k [2**(1/2) Vs t]**(2/3)
1.2
1.0
0.8
0.6
0.4
0.2
0.0
0
1
2
3
4
5

Heat mode to leading order does not couple to a pair of heat modes, but only to couple of equal type sound modes. Therefore heat conduction coeffient behaves differently from sound damping constant, because pair of sound modes in resting frame oscillates as exp(σi$c_0$kt).

Main results:

$$S_H(k,t) = \exp(-D_T(k)k^2\,|\,t\,|)$$

$$\lambda(k) = nC_p D_T(k) = nC_p\,\frac{2.1056\,(V_H^{\sigma\sigma})^2}{2^{1/3}(V_\sigma^{\sigma\sigma})^{2/3}\,(c_0 k)^{1/3}}$$

$$\frac{1}{L}\langle J_H(0)\,J_H(t)\rangle = nC_p\,\frac{2.1056\,(V_H^{\sigma\sigma})^2}{2^{1/3}\sqrt{3}\,\Gamma_E(1/3)\,(V_\sigma^{\sigma\sigma})^{2/3}\,t^{2/3}}$$

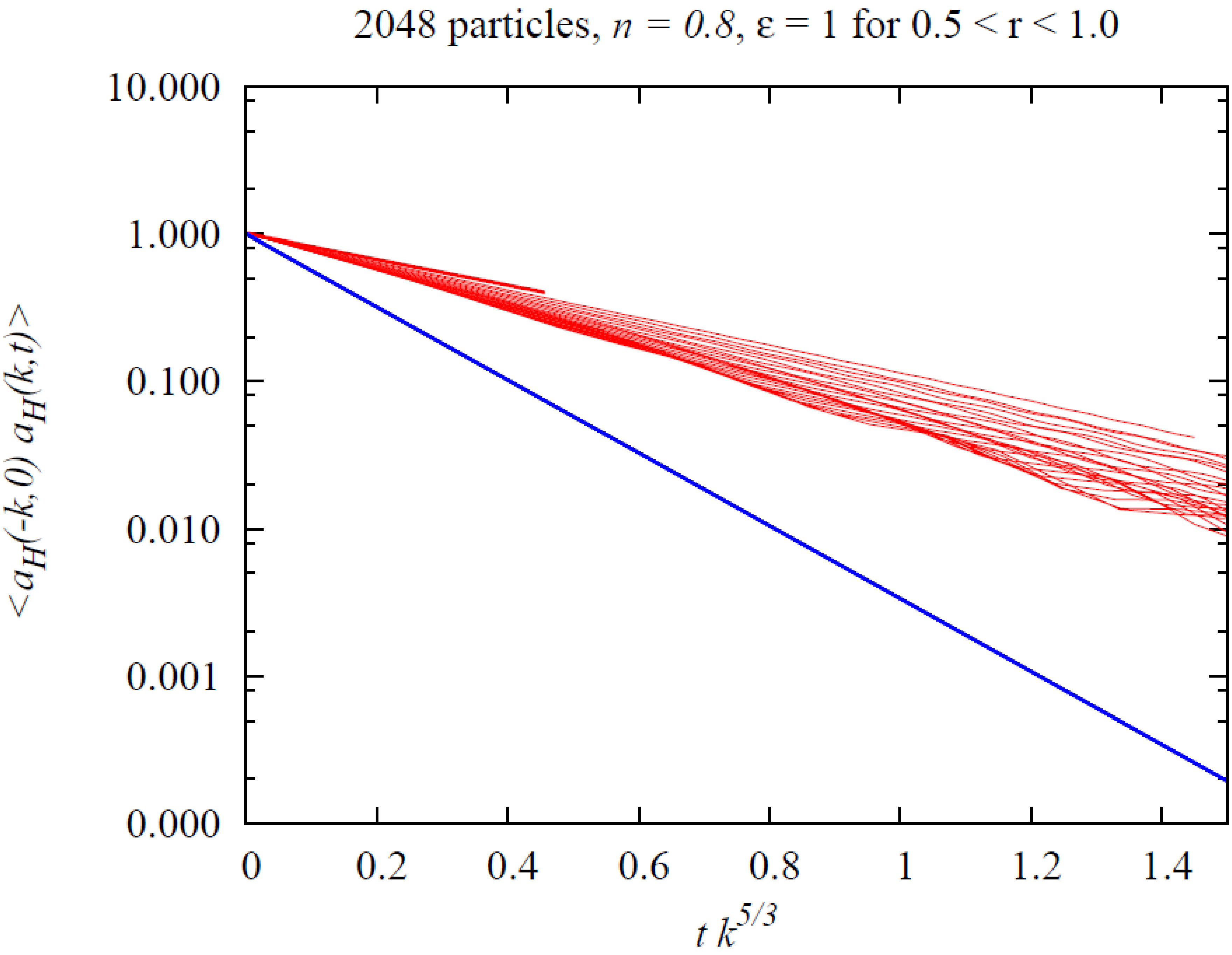

2048 particles, n = 0.8, ε = 1 for 0.5 < r < 1.0
10.000
1.000
0.100
0.010
0.001
0.000
<a_H(-k,0) a_H(k,t)>
0
0.2
0.4
0.6
0.8
1
1.2
1.4
t k^{5/3}

Mean square displacement of a tagged particle may be obtained from the collective dynamics through the identity

$$\left\langle \left(x(t)-x(0)\right)^2 \right\rangle = \frac{1}{\pi n^2}\int_{-\infty}^{\infty} dk\, \frac{\hat{S}(k,0)-\hat{S}(k,t)}{k^2}$$

with

$$\hat{S}(k,t) = \langle n(-k,0)n(k,t)\rangle$$

Explicitly:

$$\left\langle \left(x(t)-x(0)\right)^2 \right\rangle = \frac{t}{\beta mnc} + \frac{2k_B}{\pi nc_p}\Gamma_E(3/5)\alpha^{3/5}t^{3/5}$$

with $\alpha = 1.0528\dfrac{\left(V_H^{\sigma\sigma}\right)^2}{\left(2c\right)^{1/3}\left(V_\sigma^{\sigma\sigma}\right)^{2/3}}$

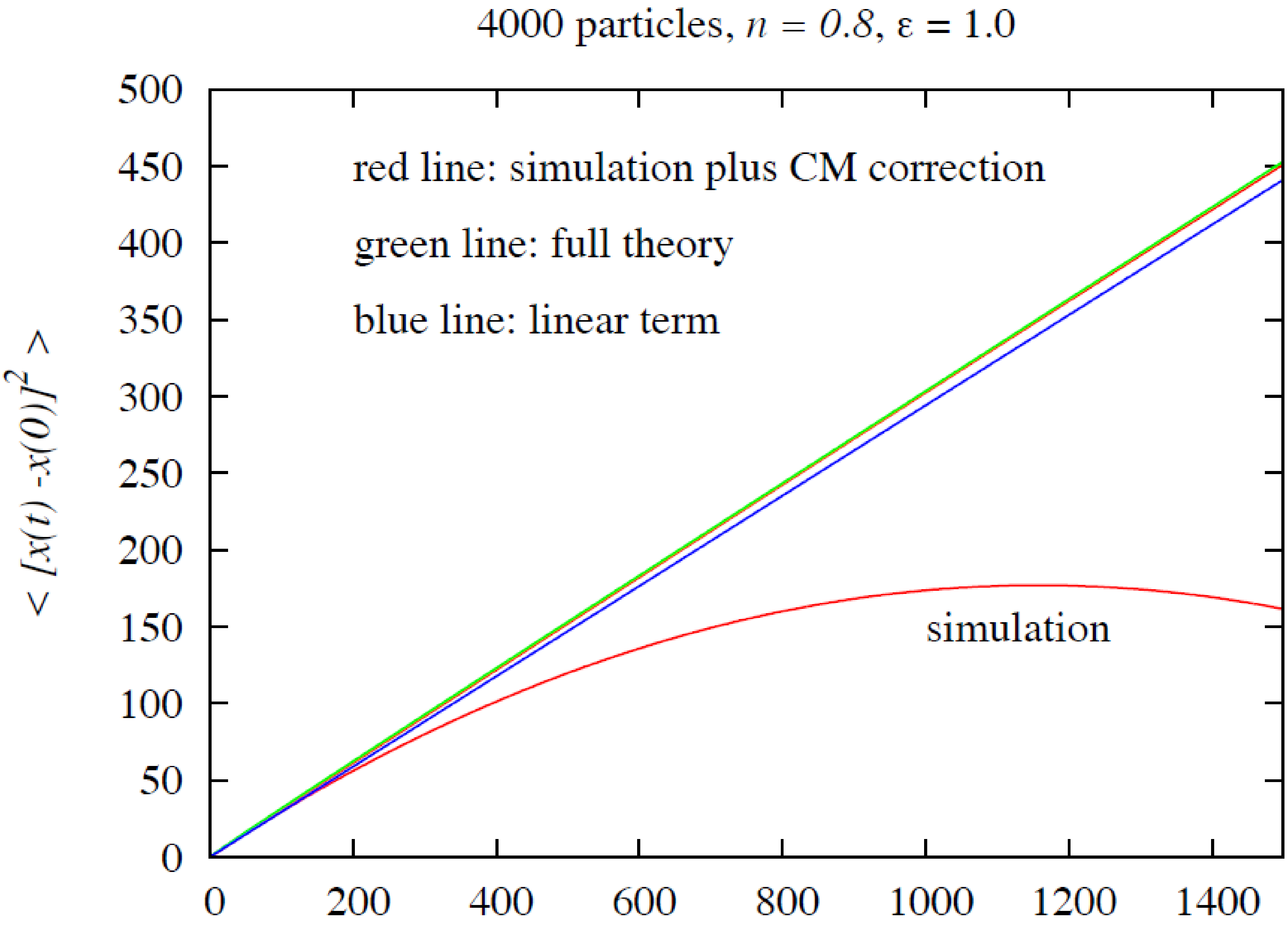

Universiteit Utrecht

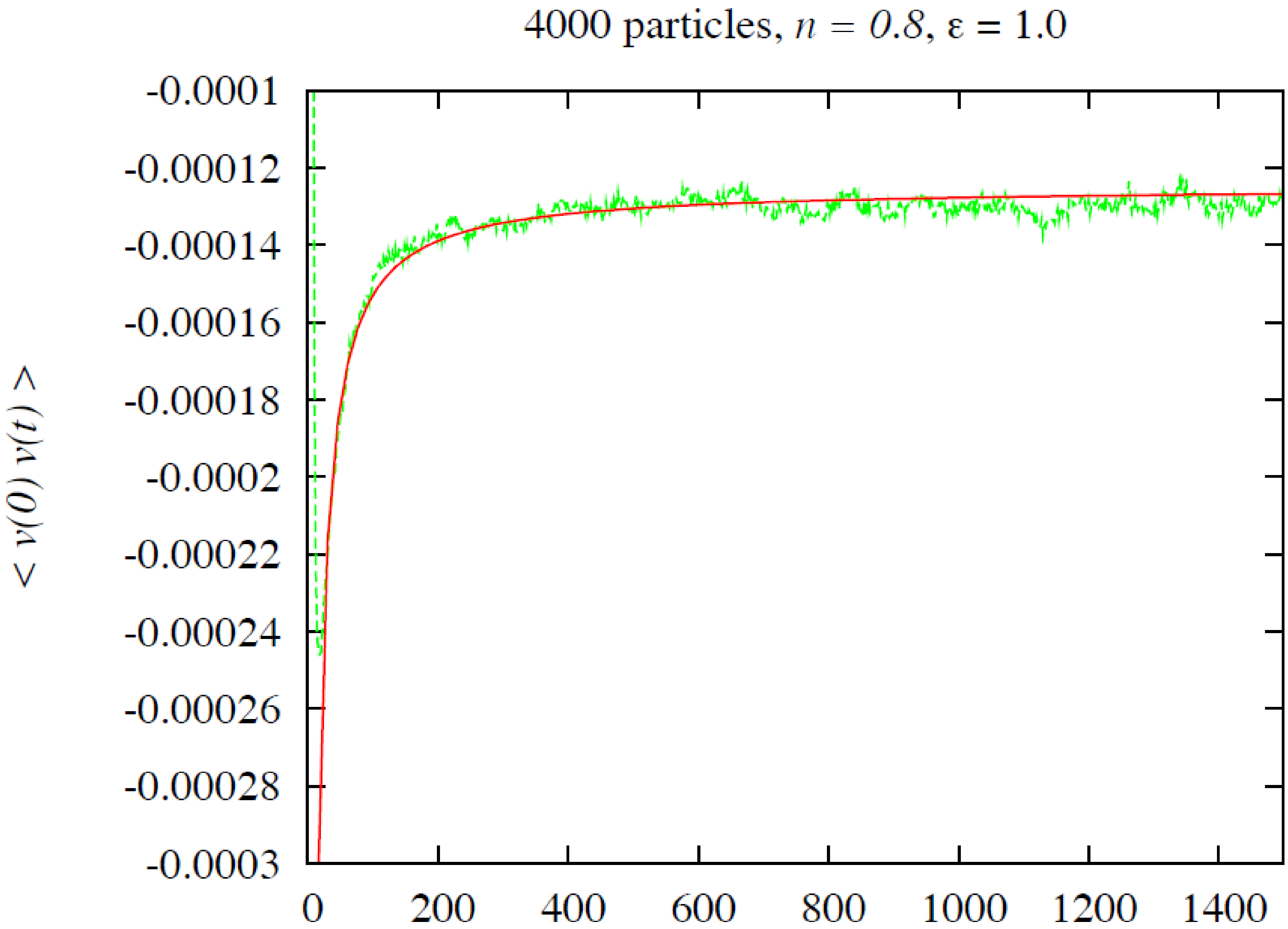

Universiteit Utrecht

Concluding remarks:

1. For typical hamiltonian systems in 1d the dominant transport properties can be expressed in terms of thermodynamic properties alone. The long time and small wave number behavior is known exactly in terms of the Prähofer-Spohn scaling functions.

2. The corrections to the leading terms are appreciable.This is because couplings of e.g. a sound mode to two opposite type sound modes or two heat modes decay only slightly faster with time than couplings to two equal type sound modes. The exponents of these correction terms can be obtained exactly, but the amplitudes only approximately.

3. Previous mode-coupling theories by Delfini et al. give a very good approximation for weakly anharmonic potentials. They require corrections otherwise, as energy density contributes to the sound modes

4. Sound damping becomes almost normal if $V_{\sigma}^{\sigma\sigma} = 0$. This happens for $\left(\frac{\partial\, c_0 n}{\partial\, n}\right)_s = 0$. In fact sound attenuation is still, logarithmically, superdiffusive. Heat conduction becomes more strongly superdiffusive. No more KPZ.

5. In spite of the diverging Green-Kubo integrals the transport coefficients in the nonlinear hydrodynamic equations need not be infinite. The long time tails in the current-current correlation functions are due to the nonlinearities in the hydrodynamic equations. Whether or not the transport coefficients in the nonlinear hydrodynamic equations are in fact divergent to my opinion is an open question.

Ref.: HvB arXiv:1106.3298v3 [cond-mat.stat-mech],
PRL 108.180601 (2012)

Universiteit Utrecht